Increasing the Curvature of a Bowl-Shaped Polyarene by Fullerene-like η2-Complexation of a Transition Metal at the Interior of the Convex Surface

ARTICLE *in* ORGANOMETALLICS · FEBRUARY 2010

Impact Factor: 4.13 · DOI: 10.1021/om100024c

5 AUTHORS, INCLUDING:

Alexander S. Filatov
University of Chicago
90 PUBLICATIONS **920** CITATIONS
SEE PROFILE

Andrey Yu Rogachev
Illinois Institute of Technology
76 PUBLICATIONS **628** CITATIONS
SEE PROFILE

Edward A Jackson
Boston College, USA
26 PUBLICATIONS **686** CITATIONS
SEE PROFILE

Lawrence T Scott
Boston College, USA
298 PUBLICATIONS **8,387** CITATIONS
SEE PROFILE

ORGANOMETALLICS
Article

Organometallics **2010,** *29,* 1231–1237 1231
DOI: 10.1021/om100024c

Increasing the Curvature of a Bowl-Shaped Polyarene by Fullerene-like η^2-Complexation of a Transition Metal at the Interior of the Convex Surface

Alexander S. Filatov,[†] Andrey Yu. Rogachev,[‡] Edward A. Jackson,[§] Lawrence T. Scott,[§] and Marina A. Petrukhina*,[†]

[†]*Department of Chemistry, University at Albany, State University of New York, Albany, New York 12222,* [‡]*Institute für Anorganische und Angewandte Chemie, Universität Hamburg, Martin-Luther-King-Platz 6, 20146 Hamburg, Germany, and* [§]*Merkert Chemistry Center, Department of Chemistry, Boston College, Chestnut Hill, Massachusetts, 02467-3860*

Received January 7, 2010

The first transition metal complex of monoindenocorannulene, $[\{Rh_2(O_2CCF_3)_4\}_2 \cdot (C_{26}H_{12})]$ (**1**), has been synthesized by gas-phase deposition and has been structurally characterized by X-ray crystallography. In the solid state, it forms a 2D organometallic network based on intermolecular Rh−C interactions and rare tetra-bridged coordination of a π-bowl. In addition to η^2-rim binding, one Rh(II) center interacts exclusively with interior carbon atoms on the convex surface, exhibiting an η^2-coordination type previously observed only in closed, all-carbon buckyballs. The latter unique coordination of Rh(II) accentuates the pyramidalization of the C atoms of monoindenocorannulene. Thus, in contrast to all other reported Rh(II) complexes with buckybowls, metal complexation leads to a curvature increase of the $C_{26}H_{12}$ core in **1**. DFT calculations (PBE0) reveal the preferred coordination sites of $C_{26}H_{12}$ to be the rim of the corannulene core, followed by the interior spoke and then the rim CC bonds of the indeno site. This calculated trend is nicely followed by the average Rh−C bond distances in the solid-state structure of **1**: 2.567 (rim) < 2.687 (spoke) < 2.715 Å (indeno site). The nature of Rh(II)−π interactions was quantitatively evaluated in terms of ligand-to-metal and metal-to-ligand contributions, showing the consistently greater role of the former in all computed complexes.

Introduction

Recent developments in the synthesis of open geodesic polyaromatic hydrocarbons (buckybowls or π-bowls)[1] have opened access to a number of curved carbon-rich molecules with different surface areas and bowl depths, including those that surpass the curvature of C_{60}.[2] Metal complexation reactions of corannulene, $C_{20}H_{10}$, the smallest nonplanar subunit of the C_{60}-fullerene, have been the major research focus both computationally[3] and synthetically.[3a,g,h,4] Despite all efforts, only three metal complexes with buckybowls having greater curvature than corannulene, namely, monoindenocorannulene,[5] sumanene,[6] and C_3-hemibuckminsterfullerene,[7] have been isolated and structurally characterized so far. Although bowl-shaped polyaromatic hydrocarbons

*Corresponding author. Fax: +1-518-442-3462. Tel: +1-518-442-4406. E-mail: marina@albany.edu.

(1) (a) Sygula, A.; Rabideau, P. W. *Carbon-Rich Compounds* **2006**, 529–565. (b) Wu, Y.-T.; Siegel, J. S. *Chem. Rev*. **2006**, *106*, 4843–4867. (c) Tsefrikas, V. M.; Scott, L. T. *Chem. Rev*. **2006**, *106*, 4868–4884.

(2) (a) Jackson, E. A.; Steinberg, B. D.; Bancu, M.; Wakamiya, A.; Scott, L. T. *J. Am. Chem. Soc*. **2007**, *129*, 484–485. (b) Steinberg, B. D.; Jackson, E. A.; Filatov, A. S.; Wakamiya, A.; Petrukhina, M. A.; Scott, L. T. *J. Am. Chem. Soc*. **2009**, *131*, 10537–10545.

(3) (a) Seiders, T. J.; Baldridge, K. K.; O'Connor, J. M.; Siegel, J. S. *J. Am. Chem. Soc*. **1997**, *119*, 4781–4782. (b) Chistyakov, A. L.; Stankevich, I. V. *J. Organomet. Chem*. **2000**, *599*, 18–27. (c) Frash, M. V.; Hopkinson, A. C.; Bohme, D. K. *J. Am. Chem. Soc*. **2001**, *123*, 6687–6695. (d) Dunbar, R. C. *J. Phys. Chem. A* **2002**, *106*, 9809–9819. (e) Kameno, Y.; Ikeda, A.; Nakao, Y.; Sato, H.; Sakaki, S. *J. Phys. Chem. A* **2005**, *109*, 8055–8063. (f) Kandalam, A. K.; Rao, B. K.; Jena, P. *J. Phys. Chem. A* **2005**, *109*, 9220–9225. (g) Siegel, J. S.; Baldridge, K. K.; Linden, A.; Dorta, R. *J. Am. Chem. Soc*. **2006**, *128*, 10644–10645. (h) Zhu, B.; Ellern, A.; Sygula, A.; Sygula, R.; Angelici, R. J. *Organometallics* **2007**, *26*, 1721–1728. (i) Rogachev, A. Y.; Sevryugina, Y.; Filatov, A. S.; Petrukhina, M. A. *Dalton Trans*. **2007**, 3871–3873. (j) Peverati, R.; Baldridge, K. K. *J. Chem. Theory Comput*. **2008**, *4*, 2030–2048. (k) Rogachev, A. Y.; Petrukhina, M. A. *J. Phys. Chem. A* **2009**, *113*, 5743–5753.

(4) (a) Alvarez, C. M.; Angelici, R. J.; Sygula, A.; Sygula, R.; Rabideau, P. W. *Organometallics* **2003**, *22*, 624–626. (b) Petrukhina, M. A.; Andreini, K. W.; Mack, J.; Scott, L. T. *Angew. Chem., Int. Ed*. **2003**, *42*, 3375–3379. (c) Vecchi, P. A.; Alvarez, C. M.; Ellern, A.; Angelici, R. J.; Sygula, A.; Sygula, R.; Rabideau, P. W. *Angew. Chem., Int. Ed*. **2004**, *43*, 4497–4500. (d) Elliott, E. L.; Hernandez, G. A.; Linden, L.; Siegel, J. S. *Org. Biomol. Chem*. **2005**, *3*, 407–413. (e) Vecchi, P. A.; Alvarez, C. M.; Ellern, A.; Angelici, R. J.; Sygula, A.; Sygula, R.; Rabideau, P. W. *Organometallics* **2005**, *24*, 4543–4552. (f) Lee, H. B.; Sharp, P. R. *Organometallics* **2005**, *24*, 4875–4877. (g) Ayers, T. M.; Westlake, B. C.; Preda, D. V.; Scott, L. T.; Duncan, M. A. *Organometallics* **2005**, *24*, 4573–4578. (h) Choi, H.; Kim, C.; Park, K.-M.; Kim, J.; Kang, Y.; Ko, J. *J. Organomet. Chem*. **2009**, *694*, 3529–3532. (i) Maag, R.; Northrop, B. H.; Butterfield, A.; Linden, A.; Zerbe, O.; Lee, Y. M.; Chi, K.-W.; Stang, P. J.; Siegel, J. S. *Org. Biomol. Chem*. **2009**, *7*, 4881–4885.

(5) Filatov, A. S.; Jackson, E. A.; Scott, L. T.; Petrukhina, M. A. *Angew. Chem., Int. Ed*. **2009**, *48*, 8473–8476.

(6) (a) Amaya, T.; Sakane, H.; Hirao, T. *Angew. Chem., Int. Ed*. **2007**, *46*, 8376–8379. (b) Petrukhina, M. A. *Angew. Chem., Int. Ed*. **2008**, *47*, 1550–1552. (c) Sakane, H.; Amaya, T.; Moriuchi, T.; Hirao, T. *Angew. Chem., Int. Ed*. **2009**, *48*, 1640–1643.

(7) Petrukhina, M. A.; Andreini, K. W.; Peng, L.; Scott, L. T. *Angew. Chem., Int. Ed*. **2004**, *43*, 5477–5481.

Published on Web 02/10/2010

persistently prefer metal binding at the edges on their surfaces, we have recently isolated the first metal complexes with single[8] and multiple[5] metal coordinations to their interior hub carbon atoms.

Annulation of five-membered rings to a nonplanar polyarene is a general way to further increase its curvature and surface area. Two general procedures have been developed for the indenoannelation of polycyclic π-systems: a Suzuki–Heck-type coupling cascade introduced by Scott and de Meijere[9] and a formal [(2+2)+2] cycloaddition to *peri*-diethynyl corannulene derivatives developed in Siegel's group.[10] In 2009, Scott's group accomplished the synthesis of the whole family of indenocorannulenes, including the preparation of monoindenocorannulene, $C_{26}H_{12}$.[2b] We have completed the X-ray structural characterization[2b] of $C_{26}H_{12}$ to illustrate that addition of one indeno group causes a bowl depth increase at the corannulene core to 1.065 Å from 0.870 Å in corannulene[11] (at 173 K). Plus, while bowl-to-bowl inversion of $C_{20}H_{10}$ is relatively fast,[12] it was shown that hexa-substituted indenocorannulenes exist as static bowls with inversion barriers higher than 24 kcal/mol,[10] and this makes them very interesting rigid π-ligands for metal binding reactions.

We have long been interested in the use of a solvent-free environment for complexation, since it prevents solvent competition for coordination and allows controlled utilization of weak but directional metal π-arene interactions.[13] The synthetic approach developed is based on the sublimation of volatile electrophilic mono- or polynuclear metal complexes in the presence of aromatic ligands. In particular, dirhodium(II,II) tetratrifluoroacetate ($[Rh_2(O_2CCF_3)_4]$ or $[Rh_2]$) has been used as an electrophilic probe to test coordination preferences of several bowl-shaped polyarenes. As a result, the first complexes of corannulene,[4b] bromocorannulene,[14] dibenzo[*a*,*g*]corannulene,[15] and the C_3-hemibuckminsterfullerene[7] have been isolated and structurally characterized. In all the above cases, the Rh_2 units demonstrate an exclusive preference for η^2-binding at the rim carbon atoms, eluding coordination to the interior part of a bowl surface.[13,16] Herein, monoindenocorannulene ($C_{26}H_{12}$, Figure 1) has been selected for coordination studies. It is a rigid bowl with an overall depth of 1.991(4) Å and both planar (indeno site) and nonplanar (corannulene core) parts, which makes $C_{26}H_{12}$ a distinctive π-ligand for further assessments of coordination preferences of open geodesic polyaromatic hydrocarbons.

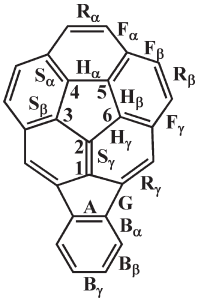

Figure 1. Assigned bond types in monoindenocorannulene: R = rim; F = flank; S = spoke; H = hub; G = gable; A = ace; B = fused benzene ring.

Results and Discussion

Sublimation–deposition of the volatile reacting partners at 205 °C under reduced pressure resulted in the formation of the monoindenocorannulene complex, $[\{Rh_2(O_2CCF_3)_4\}_2\cdot(C_{26}H_{12})]$ (**1**), having a 2:1 stoichiometry of $[Rh_2]$ to the polyarene, as indicated by elemental analysis. Multiple attempts to change the product composition by varying the reagent ratios and/or reaction temperatures did not afford any other crystalline complexes with $C_{26}H_{12}$. This contrasts with the reactivities of corannulene[4b] and monobromocorannulene,[14] where two products with different metal-to-ligand ratios ($[Rh_2]$:L = 1:1 and 3:2 in both cases) have been synthesized under controlled experimental conditions. When dark green crystals of **1** are immersed in chloroform, they slowly dissociate into starting materials, releasing free $C_{26}H_{12}$ and $[Rh_2(O_2CCF_3)_4]$, as confirmed by ^1H and ^{19}F NMR spectroscopy. The IR spectrum of **1** contains strong absorption bands of symmetric and antisymmetric stretches for the carboxylic groups of $[Rh_2(O_2CCF_3)_4]$ and weak C–H stretches of $C_{26}H_{12}$ (Figure S1, Supporting Information). The C–H stretching vibrations of the coordinated monoindenocorannulene appear at 3053, 3041, 2960, 2922, and 2852 cm^{-1} compared to those of the free ligand at 3046, 3031, 2955, 2922, and 2853 cm^{-1}. Additionally, free $C_{26}H_{12}$ has two out-of-plane C–H bending vibrations (764 and 816 cm^{-1}) that are assigned to the indeno site and the corannulene core, respectively. In **1**, these signals are shifted to 772 and 837 cm^{-1}, suggesting the metal coordination to both nonplanar and planar subunits of the hydrocarbon. Also, there is a weak band at 1708 cm^{-1} in **1**. Taking into account that the band at 1694 cm^{-1} is assigned to the almost pure stretching vibration of the CC bond connecting two five-membered rings in free monoindenocorannulene (S_γ, Figure 1), the noticeable shift observed in the IR spectrum of $[\{Rh_2(O_2CCF_3)_4\}_2\cdot(C_{26}H_{12})]$ suggests metal interaction with the interior surface of $C_{26}H_{12}$.

The single-crystal X-ray diffraction study of **1** has confirmed the above IR spectroscopy assignments and revealed the formation of an infinite 2D layered structure built on intermolecular η^2 Rh–C interactions and tetrabridged coordination of $C_{26}H_{12}$ (Figure 2).

Four metal centers from three crystallographically independent dirhodium units are coordinated to each $C_{26}H_{12}$ bowl. This type of metal binding to a π-bowl has been previously seen only in the complex of the C_3-hemifullerene,

(8) Petrukhina, M. A.; Sevryugina, Y.; Rogachev, A. Y.; Jackson, E. A.; Scott, L. T. *Angew. Chem., Int. Ed.* **2006**, *45*, 7208–7210.
(9) (a) Wegner, H. A.; Scott, L. T.; de Meijere, A. *J. Org. Chem.* **2003**, *68*, 883–887. (b) Wegner, H. A.; Reisch, H.; Rauch, K.; Demeter, A.; Zachariasse, K. A.; de Meijere, A.; Scott, L. T. *J. Org. Chem.* **2006**, *71*, 9080–9087. (c) de Meijere, A.; Stulgies, B.; Albrecht, K.; Rauch, K.; Wegner, H. A.; Hopf, H.; Scott, L. T.; Eshdat, L.; Aprahamian, I.; Rabinovitz, M. *Pure Appl. Chem.* **2006**, *78*, 813–830. (d) Quimby, J. M.; Scott, L. T. *Adv. Synth. Catal.* **2009**, *351*, 1009–1013.
(10) Wu, Y.-T.; Hayama, T.; Baldridge, K. K.; Linden, A.; Siegel, J. S. *J. Am. Chem. Soc.* **2006**, *128*, 6870–6884.
(11) (a) Hanson, J. C.; Nordman, C. E. *Acta Crystallogr.* **1976**, *B32*, 1147–1153. (b) Petrukhina, M. A.; Andreini, K. W.; Mack, J.; Scott, L. T. *J. Org. Chem.* **2005**, *70*, 5713–5716.
(12) Scott, L. T.; Hashemi, M. M.; Bratcher, M. S. *J. Am. Chem. Soc.* **1992**, *114*, 1920–1921.
(13) Petrukhina, M. A. *Coord. Chem. Rev.* **2007**, *251*, 1690–1698.
(14) Filatov, A. S.; Petrukhina, M. A. *J. Organomet. Chem.* **2008**, *693*, 1590–1596.
(15) Petrukhina, M. A.; Andreini, K. W.; Tsefrikas, V. M.; Scott, L. T. *Organometallics* **2005**, *24*, 1394–1397.
(16) Petrukhina, M. A.; Scott, L. T. *Dalton Trans.* **2005**, 2969–2975.

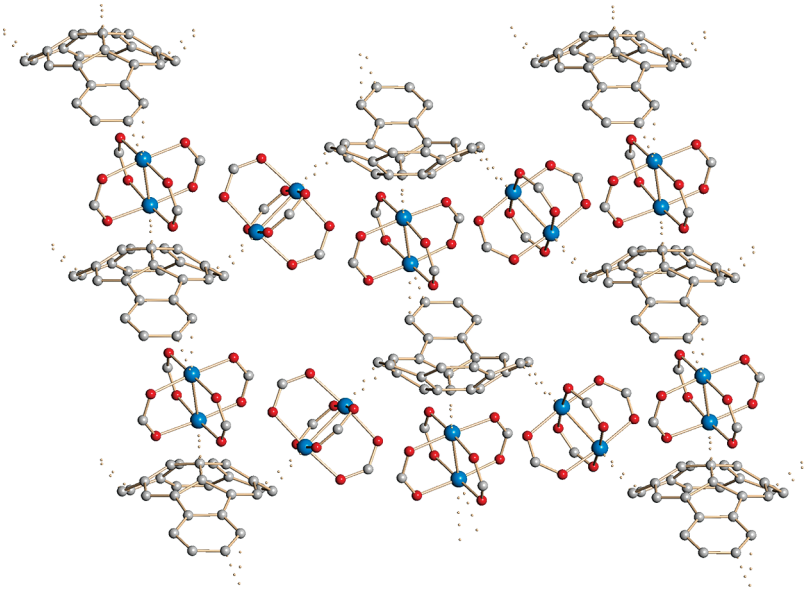

Figure 2. Part of a 2D organometallic network in the crystal structure of **1**. The CF_3 groups and H atoms are omitted for clarity.

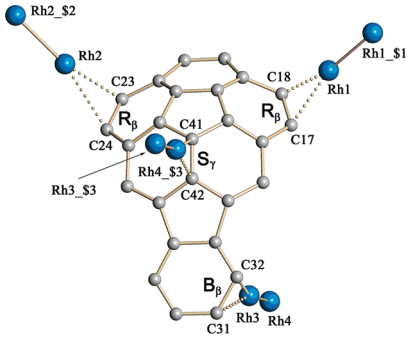

Figure 3. Tetradentate μ^4-η^2:η^2:η^2:η^2 coordination of $C_{26}H_{12}$ in **1**. Only metal centers of $[Rh_2(O_2CCF_3)_4]$ are shown for clarity. Distances (Å): Rh1−Rh1_$1 2.4275(6), Rh2−Rh2_$2 2.4330(6), Rh3−Rh4 2.4252(4), Rh1−C17 2.478(4), Rh1−C18 2.578(4), Rh2−C23 2.538(4), Rh2−C24 2.673(4), Rh3−C31 2.792(4), Rh3−C32 2.638(4), Rh4_$3−C41 2.718(4), Rh4_$3−C42 2.656(4). Atoms marked with the $ sign are at the symmetry positions $1: $-x+1, -y+2, -z+1$; $2: $-x+2, -y+2, -z$; $3: $x+1, y, z$.

which has a larger surface and a deeper bowl.[7] Similarly, three rhodium atoms in **1** approach the monoindenocorannulene ligand from the convex side, and only one is bound to the concave surface (Figure 3). However, in contrast to the 2D layered structure of $[\{Rh_2(O_2CCF_3)_4\}_2\cdot(C_{26}H_{12})]$, the hemifullerene complex exhibits an interpenetrated 3D structure with a 3:1 ratio of Rh_2 and $C_{30}H_{12}$. It is also worth noting that the tetrabridged coordination of a polyaromatic hydrocarbon seen in **1** is rare and was previously reported only in the dirhodium complex of planar chrysene.[17]

For the rhodium atoms bound to the rim carbon atoms (R_β), the Rh−C_{rim} distances are averaged at 2.528(4) and 2.606(4) Å for Rh1 and Rh2, respectively. These two dirhodium units are exclusively attached to the convex surface of the corannulene core of $C_{26}H_{12}$, using both of their axial positions. The resulting Rh−π interactions are responsible for the formation of a 1D polymeric chain along the [011] direction as part of a 2D layered network. The third Rh_2 unit is coordinated to the concave side of the indeno site (B_β), with the bonding Rh3−C distances being 2.638(4) and 2.792(4) Å. The second rhodium atom (Rh4) of the same dimetal unit is η^2-bound to the spoke carbon atoms (S_γ) of the interior part of $C_{26}H_{12}$. The Rh4−C distances are 2.656(4) and 2.718(4) Å (Figure 4).

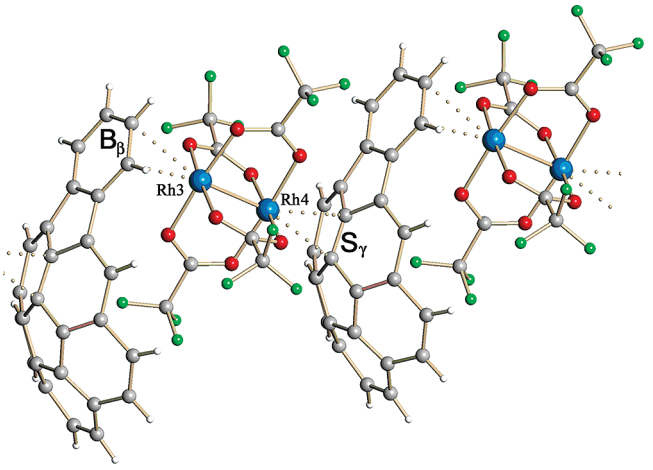

Figure 4. Fragment of a 2D network in **1** showing the coordination of the Rh_2 units to both the convex (interior spoke carbon atoms, S_γ) and concave (rim carbon atoms, B_β) surfaces of $C_{26}H_{12}$.

All previously reported complexes of $[Rh_2(O_2CCF_3)_4]$ with π-bowls have shown exclusive coordination of rhodium(II) centers to the rim carbon atoms.[7,13,16] The η^2-metal binding of Rh(II) to the interior spoke carbon site S_γ of the convex face of $C_{26}H_{12}$ in **1** is the first example of such coordination. Indeed, reactions of any sort at interior carbon atoms of polyarenes are rare.[18] Fullerenes are known

(17) Cotton, F. A.; Dikarev, E. V.; Petrukhina, M. A. *J. Am. Chem. Soc.* **2001**, *123*, 11655–11663.

(18) (a) Preda, D. V.; Scott, L. T. *Tetrahedron Lett.* **2000**, *41*, 9633–9637. (b) Bronstein, H. E.; Scott, L. T. *J. Org. Chem.* **2008**, *73*, 88–93.

Table 1. Selected Geometric Characteristics of $C_{26}H_{12}$ in Free and Coordinated Forms[a]

bond type	$C_{26}H_{12}$	**1** (X-ray)	**1** (DFT)
rim (R_α and R_γ)	1.378(4)	1.383(6)	1.398
rim (R_β)	1.379(4)	1.384(5)	1.425
flank	1.445(3)	1.445(5)	1.454
hub (H_β and H_α)	1.418(4)	1.426(6)	1.436
hub (H_γ)	1.408(4)	1.437(6)	1.435
spoke (S_α and S_β)	1.386(4)	1.383(6)	1.404
spoke (S_γ)	1.356(4)	1.357(6)	1.396
gable (G)	1.492(6)	1.479(6)	1.483
ace (A)	1.430(4)	1.431(5)	1.444
fused benzene ring (B_α and B_γ)	1.386(4)	1.389(6)	1.405
fused benzene ring B_β	1.397(4)	1.386(6)	1.409
POAV (1)	6.7	7.6	8.4
POAV (2)	11.2	12.5	12.4
POAV (3)	10.0	10.3	10.3
POAV (4)	9.8	10.1	9.2
POAV (5,6)	8.8	9.5	9.3
bowl depth[b]	1.065(4)	1.148(6)	1.156

[a] Bond distances (Å) are averaged, and π-orbital axis vector angles (POAV) are in degrees (deg). [b] The "bowl depth" is taken as the distance (Å) from the five-membered ring hub to the mean plane of the 10 carbon atoms on the rim of the corannulene core.

to prefer η^2-binding of metal centers and cycloaddition reactions at the junction of the two six-membered rings on their surfaces,[19] with the latter corresponding to the "spoke" bond of corannulene and monoindenocorannulene. Thus, the formation of $[\{Rh_2(O_2CCF_3)_4\}_2\cdot(C_{26}H_{12})]$ in this work confirms for the first time the similarity between the convex carbon surfaces of π-bowls and fullerenes in metal binding reactions. It is interesting to note that a previously reported Ru(I) complex exhibited η^1-hub-coordination of corannulene,[8] while binding the C_{60}-fullerene in a symmetrical η^2-fashion.[3i] Thus, the enlarged surface area in monoindenocorannulene compared to corannulene represents a better model of the fullerene surface properties.

A comparison between the geometric parameters of coordinated and free $C_{26}H_{12}$ shows little perturbations of the bond distances upon complexation, if statistical deviations are taken into account (Table 1).

It can be seen, however, that coordination of Rh(II) to the interior of $C_{26}H_{12}$ greatly affects the pyramidalization of the C atoms. The π-orbital axis vector (POAV) analysis of Haddon[20] is commonly used as a quantitative evaluation method for the degree of pyramidalization for trigonal C atoms. As reference points, the planar-trigonal atom is taken with a POAV angle of 0.0°, whereas the highly pyramidalized carbon atoms of the C_{60}-fullerene have POAV angles of 11.6°. The most pyramidalized carbon atom in free $C_{26}H_{12}$ has a POAV angle equal to 11.2° (Table 1). Upon metal coordination, this POAV angle is increased to 12.5°, surpassing the curvature of C_{60} and reaching that of the highly curved pentaindenocorannulene (POAV averaged for all hub C atoms is 12.6°)[2], having four more five-membered rings than $C_{26}H_{12}$. All other C atoms forming the interior bowl surface also become more pyramidalized in **1**. As a consequence, the bowl depth of $C_{26}H_{12}$ is increased in comparison with its free form (Δ = 0.08 Å). In contrast to **1**, rim binding of the same dirhodium units to other buckybowls results in the flattening of their curved surfaces (Table 2). A flattening of the corannulene core was also observed in η^6-complexes of Ir(I) and Rh(I),[3g] approaching an almost planar conformation in the extreme case of $[(Cp^*Ru)_2(\mu^2\text{-}\eta^6\text{:}\eta^6\text{-}C_{20}H_{10})][SbF_6]_2$.[3h]

Table 2. Selected Bond Distances in the [Rh_2] Complexes with Corannulene, $C_{20}H_{10}$ (μ^2-η^2:η^2 and μ^3-η^2:η^2:η^2),[4b] Dibenzo-[*a*,*g*]corannulene, $C_{28}H_{14}$ (μ^3-η^2:η^2:η^2),[15] the C_3-Hemifullerene, $C_{30}H_{12}$ (μ^4-η^2:η^2:η^2:η^1),[7] and Monoindenocorannulene, $C_{26}H_{12}$ (μ^4-η^2:η^2:η^2:η^2)[a]

	$C_{20}H_{10}$	$C_{28}H_{14}$	$C_{30}H_{12}$	$C_{26}H_{12}$
Rh−Rh (unligated)[21] 2.382(1)	2.426(1)	2.427(1)	2.42(1)	2.429(1)
Rh−C_{rim} corannulene core convex surface	2.609(4)	2.577(4)	2.50(4)	2.567(4)
Rh−C_{rim} corannulene core concave surface	2.575(4)	2.591(4)	2.54(4)	
Rh−C fused benzene rings		2.698(4)		2.715(4)
Rh−C interior surface				2.687(4)
bowl depth (complex, free bowl)	0.849(6) 0.870(2)	0.770(9) 0.830(3)	2.47(4) 2.41(4)	1.148(6) 1.065(4)

[a] All bond distances are averaged.

Theoretical Analysis of Geometrical and Electronic Structures of the [Rh_2]-Monoindenocorannulene Complexes. In order to predict the metal coordination site on an aromatic surface, an examination of frontier molecular orbital topologies and an evaluation of carbon−carbon bond orders of the multidentate π-ligand are needed.[3k,17,22] In corannulene, the two highest occupied molecular orbitals (HOMOs) are degenerate, as also are the two lowest unoccupied molecular orbitals (LUMOs).[8] Indenoannulation at the corannulene core results in a significant perturbation of the electronic structure of $C_{26}H_{12}$ (Figure S2, Supporting Information). The HOMO of monoindenocorannulene lies higher (−0.2395 vs −0.2250 au) and the LUMO is lower (−0.0658 vs −0.0830 au) than those of corannulene. Thus, the $\Delta E_{HOMO-LUMO}$ gap of $C_{26}H_{12}$ is significantly reduced in comparison with that of $C_{20}H_{10}$ (3.86 vs 4.73 eV), rendering it to be a softer ligand. The rim of the corannulene core in $C_{26}H_{12}$ is comprised of the C−C bonds with the highest bond orders: $R_\alpha(1.64) \approx R_\beta(1.63) > R_\gamma(1.54)$. Bond orders of the spoke and indeno sites are lower: $S_\gamma(1.36) \approx S_\alpha(1.35) \approx S_\beta(1.33)$, $B_\alpha(1.45) \approx B_\beta(1.42) = B_\gamma(1.42) > A(1.29)$.

For the next step, a set of monoadducts with different coordination sites, [Rh_2-η^2-$C_{26}H_{12}$] (Figure 5), has been computed, and these reveal that the rim isomer is the most energetically favorable (Table 3). This conclusion is also consistent with the above bond order estimations and the experimentally observed Rh−C bond distances in the solid-state structure of **1** (2.567 (rim) < 2.687 (spoke) < 2.715 Å (indeno site)). The bonding energy of the spoke isomer (S_γ) is ca. 2.5 kcal/mol lower than that of the rim isomer (R_β), and the coordination to the indeno site (B_β) from either the convex or the concave side is even less energetically favorable. A similar trend was observed for the rim and spoke [Rh_2] adducts with corannulene.[3k]

The description of bonding in terms of ligand-to-metal and metal-to-ligand interactions and its quantification through the second-order perturbation energy in the NBO

(19) (a) Fagan, P. J.; Calabrese, J. C.; Malone, B. *Acc. Chem. Res.* **1992**, *25*, 134–142. (b) Balch, A. L.; Olmstead, M. M. *Chem. Rev.* **1998**, *98*, 2123–2165. (c) Lee, K.; Song, H.; Park, J. T. *Acc. Chem. Res.* **2003**, *36*, 78–86.

(20) Haddon, R. C. *J. Am. Chem. Soc.* **1990**, *112*, 3385–3389.

(21) Cotton, F. A.; Dikarev, E. V.; Feng, X. *Inorg. Chim. Acta* **1995**, *237*, 19–26.

(22) Filatov, A. S.; Rogachev, A. Y.; Petrukhina, M. A. *Cryst. Growth Des.* **2006**, *6*, 1479–1484.

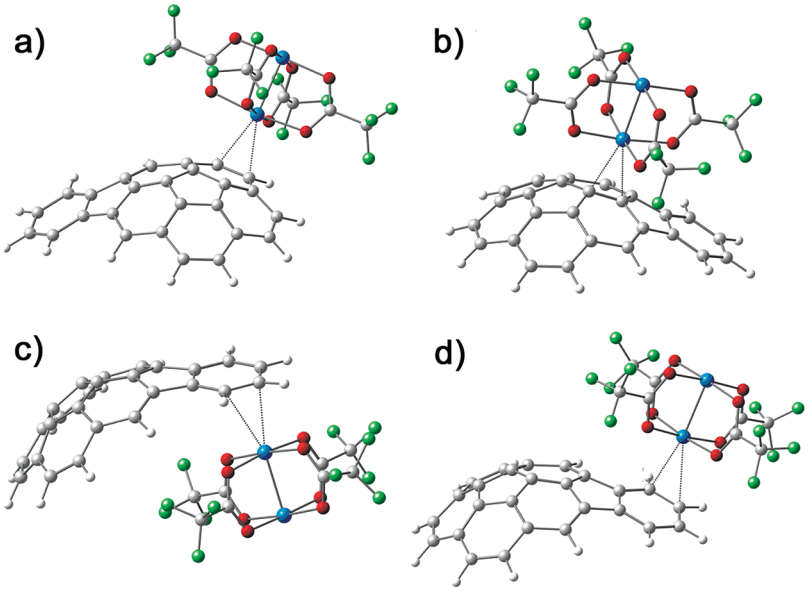

Figure 5. Equilibrium geometry configurations of monoadducts with $[Rh_2(O_2CCF_3)_4]$ coordinated to (a) R_β, (b) S_γ, (c) B_β (concave), and (d) B_β (convex) sites.

Table 3. Selected Calculated Parameters (kcal/mol) for the Monoadducts, [Rh_2-η^2-$C_{26}H_{12}$]

		$E^{(2)}_{i\rightarrow j^*}$		
monoadduct	$E_{bonding}$	M→L	L→M	∑
R_β	16.00	11.22	57.78	69.00
S_γ	13.46	9.43	49.72	59.15
B_β (concave)	11.83	7.08	34.61	41.69
B_β (convex)	12.39	8.14	35.62	43.76

basis ($E^{(2)}_{i\rightarrow j^*}$(M→L) and ($E^{(2)}_{i\rightarrow j^*}$(L→M))[23] shows that both L→M and M→L follow the same trend as the total bonding energy ($R_\beta > S_\gamma > B_\beta$ (convex or concave)). It is noteworthy that the L→M contribution greatly dominates (ca. 5 times) over M→L in all cases (Table 3).

Surprisingly, the calculated Rh−C_{hub} bond length for coordination at the S_γ site is shorter than that of the Rh−C_{spoke} bond (2.463 vs 2.658 Å). This deviates significantly from our structural data, which show that Rh−C_{hub} is longer than Rh−C_{spoke} (2.718(4) vs 2.656(4) Å). Intrigued by the observed disagreement, we carried out additional DFT computations for the bis-adducts R_β-S_γ and R_β-R_β, as well as for the tris-adduct R_β-S_γ-R_β (Figure 6).

It was found that the first coordination at the R_β site of $C_{26}H_{12}$ perturbs the electron density so that the subsequent rhodium coordination should be directed only to the corannulene core at either rim or spoke CC bonds, with the free R_β site being the most plausible, having the highest bond order (Figure 7).

Calculations of bonding energies of both R_β-R_β and R_β-S_γ adducts confirm the prediction and reveal the 1.88 kcal/mol preference for the former. The obtained bonding energies, as well as the energies of donor−acceptor interactions of bis-adducts, are decreased in comparison with monoadducts (Table S1, Supporting Information). The computed Rh−C_{hub} bond length in the R_β-S_γ bis-adduct is slightly elongated compared to the monoadduct but is still shorter than Rh−C_{spoke}. Only calculations of the tris-adduct having three $[Rh_2]$ units attached at the rim and spoke (R_β-S_γ-R_β) sites gratifyingly provide an accurate description of the geometrical features of **1**, including the above-mentioned experimental observation that the Rh−C_{hub} distance is longer than Rh−C_{spoke} (2.667 and 2.589 vs 2.718(4) and 2.656(4) Å). Thus, the elongation of the Rh−C_{hub} bond length in **1** is clearly a consequence of steric repulsive interactions of the CF_3 groups of trifluoroacetate ligands, rather than some particular electronic feature of monoindenocorannulene. Binding of each subsequent $[Rh_2]$ unit to the surface of $C_{26}H_{12}$ reduces the overall bonding energies and the energies of donor−acceptor interactions of the resulting complexes. This is attributed to a substantial decrease of the L→M and, to a lesser degree, the M→L contribution to bonding. Overall, the nature of Rh−C bonding is similar in all computed mono-, bis-, and tris-adducts with one exception. The noticeable difference in the Rh−C_{hub} and Rh−C_{spoke} bond distances in the S_γ isomer shows that the coordination may be better described as being closer to η^1 rather than η^2. This can be illustrated by the comparison of the calculated POAV angles of the C atoms 1 and 2 (Figure 1, Table 4).

Spoke coordination in S_γ increases POAV(2) to 12.5° but leaves POAV(1) unchanged, showing that interaction between Rh and C_{spoke} is relatively weak in this monoadduct. In contrast, in the R_β-S_γ-R_β tris-adduct POAV(1) is substantially increased, while POAV(2) is the same as in the S_γ isomer. Subsequently, the bowl depth of $C_{26}H_{12}$ is most greatly affected in the calculated R_β-S_γ-R_β isomer and is almost unaffected by rim coordination. Thus the calculations explicitly support the largest effect on the bowl depth caused by η^2-coordination to the interior part of the rigid monoindenocorannulene bowl.

Conclusions

The gas-phase deposition of $[Rh_2(O_2CCF_3)_4]$ with $C_{26}H_{12}$ results in the formation of $[\{Rh_2(O_2CCF_3)_4\}_2\cdot(C_{26}H_{12})]$ (**1**), the first transition metal complex of monoindenocorannulene. Unlike all previously reported rhodium(II) complexes

(23) (a) Reed, A. E.; Curtiss, L. A.; Weinhold, F. *Chem. Rev.* **1988**, *88*, 899–926. (b) Weinhold, F.; Landis, C. A. *Valency and Bonding: A Natural Bond Orbital Donor-Acceptor Perspective*; Cambridge University Press: Cambridge: 2005.

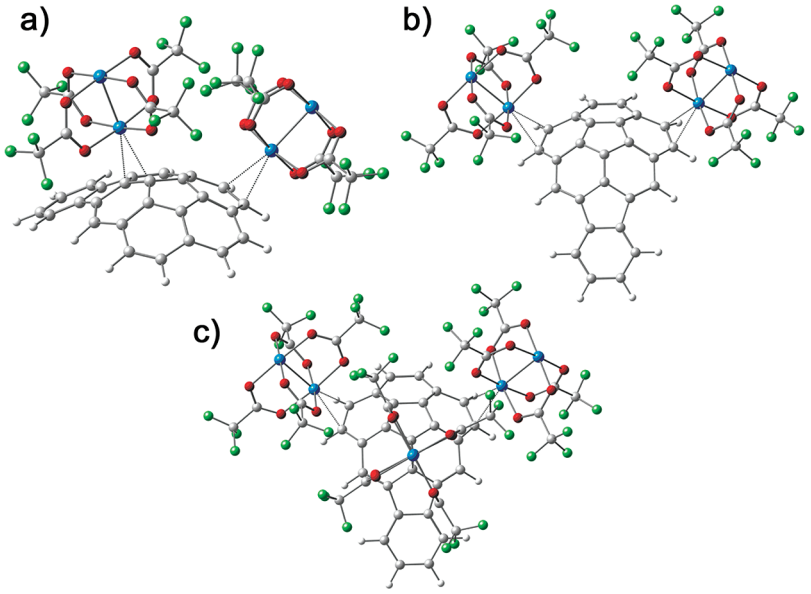

Figure 6. Equilibrium geometry configurations of bis- and tris-adducts with $[Rh_2(O_2CCF_3)_4]$ coordinated to (a) R_β-S_γ, (b) R_β-R_β, and (c) R_β-S_γ-R_β sites.

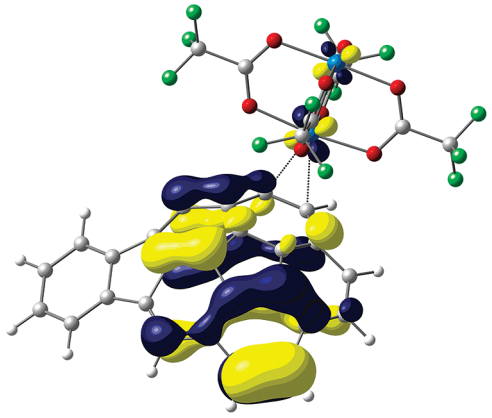

Figure 7. Active donor monoindenocorannulene-based MO in the monoadduct of $[\{Rh_2(O_2CCF_3)_4\}\cdot(C_{26}H_{12})]$ coordinated at the R_β site.

Table 4. Degree of Pyramidalization (POAV, deg) and Bowl Depth (Å) in All DFT-Computed Complexes

coordination site	POAV (1)	POAV (2)	POAV[a] (3,6)	POAV[a] (4,5)	bowl depth
free $C_{26}H_{12}$	7.0	11.1	10.0	9.1	1.076
S_γ	6.9	12.5	9.9	9.1	1.094
R_γ	6.8	11.2	9.9	9.0	1.074
B_β (concave)	7.0	11.1	10.0	9.0	1.077
B_β (convex)	6.9	11.1	9.9	9.2	1.076
R_β-R_β	6.8	11.3	10.0	9.1	1.087
R_β-S_γ	7.1	12.5	10.1	9.1	1.111
R_β-S_γ-R_β	8.4	12.5	10.2	9.2	1.156

[a] Averaged over 3 and 6, or 4 and 5.

with buckybowls, in addition to rim η^2-coordination, a metal atom is also bound to the interior part of the convex π-surface of $C_{26}H_{12}$. This new type of interaction leads to a noticeable increase of the bowl depth ($\Delta = 0.08$ Å), with the effect being similar to that provided by the annulation of one additional pentagon to a bowl. DFT calculations support the fact that the η^2-spoke coordination to the interior part of the $C_{26}H_{12}$ bowl provides the greatest effect on its curvature. The pyramidalization angles of the C atoms involved in the above coordination are substantially increased, surpassing the curvature of C_{60} for one of them. This clearly demonstrates the influence the metal coordination can cause to bowl-shaped polyarenes. It is especially noteworthy, since metal binding can likewise change the shape of other curved carbon surfaces, such as the caps or walls of carbon nanotubes, but the inapplicability of the single-crystal X-ray diffraction methods for the latter systems would prevent direct evaluation of such effects.

Experimental Section

General Procedures. All manipulations were carried out in a dry, oxygen-free, dinitrogen atmosphere by employing standard Schlenk techniques. All purchased solvents were anhydrous and freshly distilled before reactions. The synthesis of $[Rh_2(O_2CCF_3)_4]$ was carried out as previously reported.[21] Elemental analysis was performed by Maxima Laboratories Inc., Ontario, Canada. The IR spectra were recorded on a Perkin-Elmer FT-IR spectrometer (Spectrum 100) in the range 4000−600 cm^{-1} using a universal ATR sampling accessory. The NMR spectra were obtained using a Bruker Avance 400 spectrometer at 400 MHz for ^1H and at 376.47 MHz for ^{19}F. Chemical shifts are reported in ppm relative to the respective internal standards, TMS for ^1H and $CFCl_3$ for ^{19}F ($\delta = 0.0$ ppm).

Synthesis. $[\{Rh_2(O_2CCF_3)_4\}_2\cdot(C_{26}H_{12})]$ **(1).** Inside the dry-box, a mixture of $[Rh_2(O_2CCF_3)_4]$ and monoindenocorannulene, $C_{26}H_{12}$,[2b] was loaded into a small glass ampule (0.7 cm o.d.). The ratio of the dirhodium complex to the ligand was set to 3:1 (0.06 and 0.02 mmol). The ampule was sealed under vacuum (ca. 10^{-2} Torr) and placed in a tube furnace having a small temperature gradient along the length of the tube. The temperature was set at 205 °C. The dark green block-shaped crystals were deposited in one day in the coldest part of the ampule, where the temperature was set at 185 °C. Yield: 35%. Anal. Calcd for $C_{42}H_{12}F_{24}O_{16}Rh_4$: C, 30.73; H, 0.73. Found: C, 30.81; H, 0.68. IR (cm^{-1}): 3053(w), 3041(w), 2960(w), 2922(w), 2852(w), 1708(w), 1660(s), 1489(w), 1464(m), 1446(w), 1427(w), 1413(w), 1310(w), 1282(w), 1188(s), 1155(s), 1016(w),

974(w), 948(w), 888(w), 859(s), 873(m), 837(w), 802(w), 784(s), 772(w), 736(s), 714(m), 662(m). ^{1}H NMR ($CDCl_3$, ppm): 7.19−7.21 (m, 1H), 7.52 (s, 1H), 7.56 (d, J = 8.0 Hz, 1H), 7.62−7.65 (m, 3H). ^{19}F NMR ($CDCl_3$, ppm): −75.0.

X-ray Crystal Structure Determination of 1. Single crystals of $[\{Rh_2(O_2CCF_3)_4\}_2\cdot(C_{26}H_{12})]$ were picked up from the coldest end of the ampule, mounted in silicon grease, and transferred to the cold stream of the diffractometer. Several crystals were subjected to X-ray diffraction analysis, and all conformed to the same unit cell, thus confirming the homogeneity of the crystalline product obtained. The crystallographic data were collected on a Bruker AXS diffractometer equipped with a SMART CCD detector with a Mo-target X-ray tube (λ = 0.71073 Å). Cell refinement and data reduction were performed using SAINT.[24] The structure was solved by direct methods and refined by full-matrix least-squares on F^2 using the SHELXTL software package.[25] All non-hydrogen atoms were refined anisotropically except for the three disordered CF_3 groups, for which the disorder was individually modeled over three rotational orientations in each case. All hydrogen atoms were constrained to the parent carbon atoms using a riding model.

Crystal data: $Rh_4C_{42}F_{24}O_{16}H_{12}$, M = 1640.16, triclinic, a = 9.3332(4) Å, b = 13.0562(6) Å, c = 21.4259(9) Å, α = 88.150(1)°, β = 77.640(1)°, γ = 73.326(1)°, V = 2441.9(2) Å^3, T = 173 K, space group $P\bar{1}$ (no. 2), Z = 2, 10 979 reflections measured, R_1, wR_2 [$I > 2\sigma(I)$] = 0.039, 0.090; R_1, wR_2 (all data) = 0.055, 0.097, quality of fit = 1.028.

Computational Details. The geometries of all adducts were optimized at the DFT level of theory using the exchange−correlation parameters-free functional PBE0.[26] This functional has previously been successfully applied for modeling of structures and properties of curved polyaromatic systems such as nanotubes and their complexes with metal ions.[27] All starting geometries for target models have been taken as fragments of **1**. The Rh atom was described by a combination of the Stuttgart/Bonn relativistic effective core potential (RECP)[28] and the triple-ζ quality basis set developed by Weigend and Ahlrichs. It was further augmented by the two polarization functions with the following contraction scheme: (6s4p3d2f1g)/[7s7p6d2f1g] (abbreviated def2-TZVPP). The standard TZVP basis sets were used for all other atoms (C, H, O, F). The C_s and C_4 symmetry constraints were imposed for calculations of $C_{26}H_{12}$ and $[Rh_2(O_2CCF_3)_4]$, respectively. The resulting geometry configurations were tested to be true minima by calculation of full Hessian matrices and, consequently, harmonic frequencies. The lack of imaginary frequencies for each model indicated that the true minima on the potential energy surfaces were successfully achieved. Electronic structures were analyzed by the GENNBO (version 5G) program.[23] The bond orders quoted in the text were calculated in accordance with the Wiberg formulation[29] (so-called Wiberg bond indexes in natural atomic orbital basis). All calculations were carried out in the PC GAMESS/Firefly quantum chemistry program package,[30] which is partially based on the GAMESS-US source code.[31] The equilibrium geometry configurations as well as molecular orbitals were analyzed and visualized with the help of the ChemCraft program package.[32]

Acknowledgment. M.P. thanks the National Science Foundation (CHE-CAREER-0546945) for financial support and is also very grateful to the University at Albany for supporting the X-ray center at the Department of Chemistry. Research support from the Department of Energy (DE-FG02-93ER14359) and funds from the National Science Foundation (DBI-0619576) for the purchase of mass spectrometers at Boston College are also gratefully acknowledged.

Supporting Information Available: Crystallographic data for **1** given as a CIF file, computation tabular materials, and IR spectroscopy data. This material is available free of charge via the Internet at http://pubs.acs.org.

(24) *SAINT, Version 6.02*; Bruker AXS, Inc.: Madison, WI, 2001.
(25) Sheldrick, G. M. *SHELXTL, Version 6.14*; University of Gottingen, Germany, 2000.
(26) (a) Perdew, J. P.; Burke, K.; Ernzerhof, M. *Phys. Rev. Lett.* **1996**, *77*, 3865–3868. (b) Perdew, J. P.; Burke, K.; Ernzerhof, M. *Phys. Rev. Lett.* **1997**, *78*, 1396–1399.
(27) (a) Barone, V.; Peralta, J. E.; Scusseria, G. E. *Nano Lett.* **2004**, *5*, 1830–1833. (b) Johansson, M. P.; Sundholm, D.; Vaara, J. *Angew. Chem., Int. Ed.* **2004**, *43*, 2678–2681. (c) Bettinger, H. F. *J. Phys. Chem. B* **2005**, *109*, 6922–6924.
(28) Figgen, D.; Rauhut, G.; Dolg, M.; Stoll, H. *Chem. Phys.* **2005**, *311*, 227–244.
(29) Wiberg, K. B. *Tetrahedron* **1968**, *24*, 1083–1096.
(30) Granovsky, A. A. *PC GAMESS/Firefly*, v.7.1.9, http://classic.chem.msu.su/gran/gamess/index.html.
(31) Schmidt, M. W.; Baldridge, K. K.; Boatz, J. A.; Elbert, S. T.; Gordon, M. S.; Jensen, J. H.; Koseki, S.; Matsunaga, N.; Nguyen, K. A.; Su, S.; Windus, T. L.; Dupuis, J. A.; Montgomery, J. A. *J. Comput. Chem.* **1993**, *14*, 1347–1363.
(32) http://www.chemcraftprog.com.